tions in synchronization (*19*). We have performed additional simulations indicating that dendritic electroresponsiveness, such as we have used, is not required for initiation of interictal spikes if the chemical synapses are sufficiently strong. Whether signal amplification via active dendritic bursting is necessary for synchronization remains to be determined experimentally.

ROGER D. TRAUB
IBM Watson Research Center, Yorktown Heights, New York 10598, and Neurological Institute, New York 10032

ROBERT K. S. WONG
Department of Physiology and Biophysics, University of Texas Medical Branch, Galveston 77550

References and Notes

1. R. K. S. Wong and D. A. Prince, *J. Neurophysiol.* **45**, 86 (1981); ———, A. I. Basbaum, *Proc. Natl. Acad. Sci. U.S.A.* **76**, 986 (1979).
2. M. Dichter and W. A. Spencer, *J. Neurophysiol.* **32**, 649 (1969); *ibid.*, p. 663.
3. P. A. Schwartzkroin and D. A. Prince, *Ann. Neurol.* **1**, 463 (1977); *Brain Res.* **147**, 117 (1978).
4. Guinea pig transverse hippocampal slices were prepared and perfused as described (*5*). Sodium penicillin (1.7 m*M*) was included in the bathing medium. Interictal spikes, with corresponding multipeaked field potentials and simultaneous intracellular bursting, were recorded in CA2–CA3; these events occurred either spontaneously or were elicited by local stimuli. The isolated CA2–CA3 region was obtained by making a cut across the transverse slice extending from the superior alveus to the inferior alveus. The cut began at a point on the superior alveus about 1.4 mm from the fornix and ended on the inferior alveus about 1 mm from the fornix. The cut separated the CA1 cells, the granule cells, and some of the CA4 cells from the CA2–CA3 region. CA2 was isolated by making an additional cut from the alveus to the hippocampal fissure. This cut began at a point on the superior alveus about 0.7 mm from the fornix.
5. R. K. S. Wong and R. D. Traub, *J. Neurophysiol.*, in press.
6. R. D. Traub, *Neuroscience*, in press.
7. B. A. MacVicar and F. E. Dudek, *Brain Res.* **184**, 220 (1980).
8. R. K. S. Wong and D. A. Prince, *Science* **204**, 1228 (1979); R. Dingledine and L. Gjerstad, *Brain Res.* **168**, 205 (1979).
9. This model applies most directly to stimulus-evoked interictal spikes wherein the stimulus itself serves to synchronize a small group of cells. Presumably, the initial event in a spontaneous interictal spike is also the synchronous discharge of a small group of cells. The mechanism by which this initial synchronization comes about during a spontaneous interictal spike is not considered here.
10. R. D. Traub and R. K. S. Wong, *Neuroscience* **6**, 223 (1981).
11. ———, *J. Neurophysiol.*, in press.
12. E. S. Goldensohn and D. P. Purpura, *Science* **139**, 840 (1963); D. A. Prince, *Exp. Neurol.* **21**, 467 (1968); D. Johnston and T. H. Brown, *Science* **211**, 294 (1981).
13. P. A. Schwartzkroin and M. Slawsky, *Brain Res.* **135**, 157 (1977); R. K. S. Wong and D. A. Prince, *Brain Res.* **159**, 385 (1978).
14. B. E. Alger and R. A. Nicoll, *Science* **210**, 1122 (1980); J. R. Hotson and D. A. Prince, *J. Neurophysiol.* **43**, 409 (1980).
15. R. W. Aldrich, Jr., P. A. Getting, S. H. Thompson, *J. Physiol. (London)* **291**, 507 (1979).
16. D. Tillotson, *Proc. Natl. Acad. Sci. U.S.A.* **76**, 1497 (1979).
17. Parameters of this model include: R_{input} = 32 megohms; R_m = 10,000 ohm-cm^2, C_m = 3 μF/cm^2, τ_m = 30 msec, $\bar{g}_{Na}$ = 75 mS/cm^2, and the R_{input} of active dendritic branch is 90 megohms, where R_{input} is input resistance, R_m is membrane resistivity, C_m is membrane capacitance, τ_m is a membrane time constant, and $\bar{g}_{Na}$ is maximum sodium conductance. Time constants for removal of g_{Ca} inactivation and for decrease of slow K^+ conductance were different for each cell, varying from 182 to 222 msec and 446 to 571 msec, respectively. For other parameters, see (*6*). Differential equations modeling each neuron were integrated by using a second-order Taylor series with time step dt = 50 μsec. The membrane potential is not altered when dt = 33 μsec. The equations were embodied in a set of PL/I programs and run on an IBM 370 model 168 computer. A simulation of 120 msec of activity used 14.4 minutes of CPU time.
18. Synchronization in the model occurs over a range of synaptic strengths, so long as bursting can spread from cell to cell. The exact value of synaptic strength determines the time it takes for spread of bursting and hence determines the sharpness of synchronization (R. D. Traub and R. K. S. Wong, in preparation). It is reasonable to assume that bursting in one cell can indeed evoke bursting in another: a 2-msec injected current depolarizing a CA3 cell 2 to 5 mV can evoke a burst (*1*). Recurrent EPSP's larger than this have been reported (*7*), although direct comparison is difficult since in this case the postsynaptic neuron was hyperpolarized. Previous work [T. H. Brown, R. K. S. Wong, D. A. Prince, *Brain Res.* **177**, 194 (1979)] has shown that spontaneous EPSP's can depolarize CA3 cells up to 4 mV. Multiple burst initiation sites in soma and dendrites (*1*) may contribute to the spread of bursting.
19. B. A. MacVicar and F. E. Dudek, *Science* **213**, 782 (1981).
20. This model is distinguished from our earlier one (*10*) in a fundamental way; in the present model, each neuron connects only to a few other cells, rather than to 60 or more as in the earlier study. In addition, each neuron is now represented more realistically. Although the previous study showed the importance of recurrent excitation, the anatomical assumptions were less accurate than in the present model, and it was unable to reproduce field potentials of long latency.
21. W. D. Knowles and P. A. Schwartzkroin, *J. Neurosci.* **1**, 318 (1981).
22. We thank F. A. Dodge, Jr., and G. J. Lasher for reviewing the manuscript. Supported in part by NIH grant NS18464 and a Klingenstein fellowship award (to R.K.S.W.).

7 January 1982; revised 19 March 1982

New Dopaminergic and Indoleamine-Accumulating Cells in the Growth Zone of Goldfish Retinas After Neurotoxic Destruction

Abstract. *Juvenile goldfish were allowed to grow for 3 months after dopaminergic or indoleamine-accumulating cells in their retinas had been destroyed by intravitreal injection of 6-hydroxydopamine or 5,7-dihydroxytryptamine, respectively. New cells of each type were found growing in concentric rings at the margin of the retina. To compensate for the loss of dopaminergic innervation in retinas treated with 6-hydroxydopamine, cells in the growth zone appeared to proliferate at a higher rate than those in untreated retinas and long processes were extended into the retina by the first dopaminergic cells to appear.*

In histological and histochemical studies of retinal enlargement in the goldfish eye, Easter and his colleagues (*1*) found that the number of neurons per retina increases with growth while the density (except for rods) decreases (*1*, *2*). Thymidine autoradiography has demonstrated that cell proliferation leading to the formation of new neurons takes place only in the peripheral zone neighboring the ora terminalis (*2*). Therefore, new retinal tissue is added in concentric rings. Fluorescence microscopic studies of goldfish and carp retinas have revealed that, with increasing diameter of the retina, dopaminergic (DA) cells (*3*) and indoleamine-accumulating (IA) cells (*4*) also increase in number while decreasing in density (*5*). This pattern of growth is thus identical to that described for other classes of retinal cells (*2*).

In the retinas of adult carp (body length, 30 to 35 cm), DA cells are destroyed by intravitreal injection of 6-hydroxydopamine (6-OHDA), and IA cells are destroyed by 5,7-dihydroxytryptamine (5,7-DHT) (*6*). Total destruction of IA cells can be achieved by a

Table 1. Body length, eyeball diameter, retinal growth zone width, and DA and IA cell density in control goldfish and in goldfish treated with 6-OHDA or 5,7-DHT 3 months before eyeball enucleation. Growth zone width and cell density are corrected for tissue shrinkage in the fixative (*5*). Values are means ± standard errors.

Group	Body length, tip to tip (cm)	*N**	Eyeball diameter, horizontal (mm)	Growth zone width (μm)	Cells per square millimeter	
					DA	IA
6-OHDA–treated	12.0 ± 0.5	7	7.0 ± 0.1	252 ± 37	186.4 ± 54.0†	200.6 ± 53.0†
5,7-DHT–treated	12.5 ± 0.7	5	7.0 ± 0.1	251 ± 42	144.3 ± 51.9	166.6 ± 41.2
Control, end of experiment	12.3 ± 0.8	6	7.1 ± 0.1	252‡	112.6 ± 16.7	132.2 ± 13.2

*Number of retinas examined. †Significantly different from corresponding control value at $P < .02$ (Student's *t*-test). ‡Corresponds to the mean value for growth zone width in all the treated retinas.

0036-8075/82/0514-0747$01.00/0

single 15-μg injection of 5,7-DHT 2 to 3 days before enucleation of the eyeball. Furthermore, these cells remain undetectable for up to 50 days after such treatment (*7*). The rate at which DA cells die varies from preparation to preparation after intravitreal injection of 6-OHDA (15 μg) plus pargyline (15 μg) on two successive days 1 week before enucleation (*6*). However, the retinal periphery, where growth occurs, is almost always devoid of DA cells soon after such treatment, indicating that newly formed DA cells are more susceptible to the neurotoxin than more mature cells in the central retina (*6*). If the destruction of DA and IA cells in the peripheral retina is permanent but the germinal cells remain intact, this technique should be useful for measuring retinal expansion in juvenile fish in terms of the rate of proliferation of new DA or IA cells. The present study was designed to test this possibility.

Seventy juvenile goldfish (*Carassius auratus*) having a similar size were obtained from a local dealer. Initial body length (10.2 ± 0.5 cm) and eyeball diameter (6.0 ± 0.2 mm) were determined from ten of the fish designated as controls. The other fish were divided into three groups of 20. In the first group a mixture of 6-OHDA (2.5 μg) and pargyline (2.5 μg) was intravitreally injected into the right eye, in the second group 5,7-DHT (2.5 μg) was injected into the left eye, and in the third group the 6-OHDA and pargyline mixture was injected into the right eye and 5,7-DHT was injected into the left eye. The injections were given on two successive days. One week later, several fish were killed to ascertain that DA or IA cells had disappeared from the retinal periphery (*5*). The remaining fish were kept together in an aquarium under diurnal lighting for 3 months (June to September). During the period, some fish or retinas were lost to death or infection.

At the end of the 3 months, healthy surviving fish were taken at random from the aquarium. Eyeballs were enucleated and the retinas were isolated and processed with a histofluorescence method for flat mounts. To facilitate detection of the cells, a mixture of norepinephrine (0.5 μg) and 5,6-dihydrotryptamine (5,6-DHT) (0.5 μg) was intravitreally injected 2 hours before enucleation. Norepinephrine enhances green fluorescence of DA cells, while 5,6-DHT is taken up selectively by IA cells, producing a yellow fluorescence (*6*).

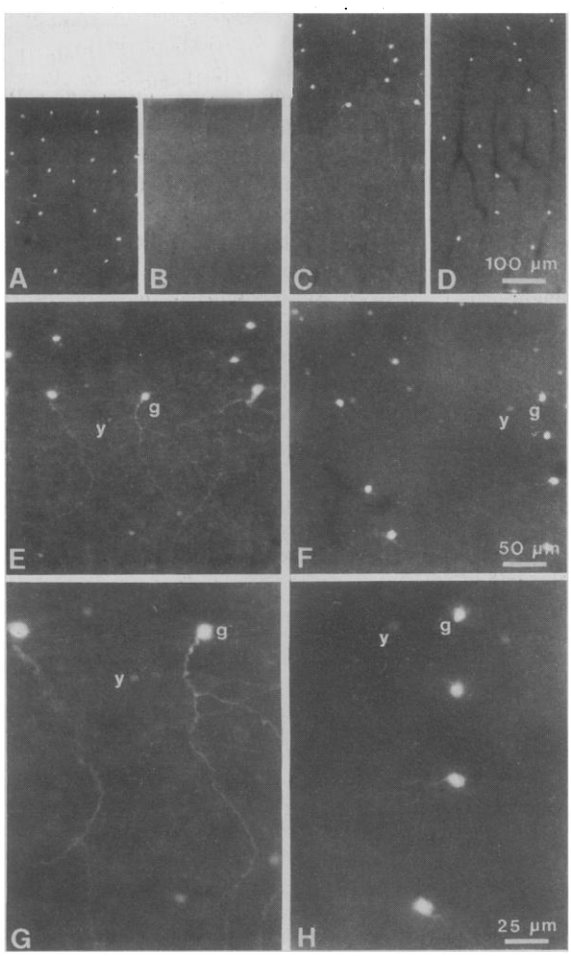

Fig. 1. (A to D) Retinal growth zone in juvenile goldfish. Fluorescence photomicrographs were taken of the peripheral region of flat mounts at low magnification. Growth zones are shown in a control retina at the beginning of the experiment (A), in retinas 1 week (B) and 3 months (C) after injection of 6-OHDA, and in a control retina at the end of the experiment (D). (E and F) Border region between newer and older parts of retinas 3 months after treatment with 6-OHDA (E) or 5,7-DHT (F). Upper parts correspond to immature tissue while lower parts correspond to more mature tissue. (G and H) Enlargements of (E) and (F). The DA cell (*g*) in (E) and (G) belongs to the group of DA cells formed earliest after injection of 6-OHDA, and the IA cell (*y*) in (F) and (H) belongs to the group of IA cells formed earliest after injection with 5,7-DHT.

Fluorescence photomicrographs (Fig. 1) show a normal retina at the beginning of the experiment, retinas 1 week and 3 months after injection of 6-OHDA, and a normal retina at the end of the experiment. The retinal margin corresponds to the upper edge of each photomicrograph. In these low-magnification views the IA cells are barely detectable. The DA cells are larger and fluoresce more intensely. In the normal retinas DA and IA cells are interspersed randomly. One week after 6-OHDA treatment, however, all the DA cells have been eliminated; the IA cells (small and weakly fluorescent) remain intact. The upper portion of Fig. 1C shows a newly formed retinal edge 3 months after 6-OHDA treatment. Here both DA and IA cells are present, but in the more mature (inner) part of the retina only IA cells are visible. Some of the more deeply situated DA cells show development as demonstrated by the appearances of processes.

Photomicrographs at higher magnifications show the borders between more mature and less mature parts of retinas treated with 6-OHDA (Fig. 1, E and G) or 5,7-DHT (F and H) 3 months before enucleation. Peripheral DA cells, which were formed first after the injection of 6-OHDA, extend long processes toward the center, where DA cells are still absent (Fig. 1, E and G). Long, centrally directed processes were never found in retinas treated with 5,7-DHT (Fig. 1, F and H) or in untreated retinas of similar size (Fig. 1D) (*5*). Rather, in such retinas the DA cell processes paralleled the retinal edge (Fig. 1H). Since the processes of IA cells are undetectable in flat mounts, possible differences in their arborization cannot be observed.

The width of the cell proliferation zone in retinas 3 months after being treated with 6-OHDA was almost the same as that in retinas treated with 5,7-DHT (251 ± 42 μm) (Table 1). The densities of DA and IA cells in the growth zone of treated retinas were compared with cell densities in a marginal zone (520 μm wide) of control retinas (Table 1). In 6-OHDA–treated retinas DA and IA cell densities were significantly higher than the corresponding control values, indicating that the proliferation rate of these cells is increased by 6-OHDA treatment. Approximately 1118 DA cells and 1204 IA cells were added in the growth zone (~ 6 mm^2) during the 3 months after treatment with 6-OHDA. The corresponding values in untreated retinas

were 676 DA cells and 793 IA cells. Therefore the proliferation rates were 12.4 DA cells and 13.4 IA cells per day in 6-OHDA–treated retinas and 7.5 DA cells and 8.8 IA cells per day in untreated retinas. At present, there is no evidence that such mitotic stimulation following cellular destruction with 6-OHDA is specific for monoaminergic cells or general for other retinal cells.

KOROKU NEGISHI
TSUNENOBU TERANISHI
SATORU KATO
Department of Neurophysiology, Neuroinformation Research Institute, University of Kanazawa School of Medicine, Kanazawa, Ishikawa 920, Japan

References and Notes

1. S. S. Easter, Jr., P. R. Johns, L. R. Baumann, *Vision Res.* **17**, 469 (1977); P. R. Johns and S. S. Easter, Jr., *J. Comp. Neurol.* **176**, 331 (1977).
2. P. R. Johns, *J. Comp. Neurol.* **176**, 343 (1977); *Am. Zool.* **21**, 447 (1981); ——— and R. D. Fernald, *Nature (London)* **293**, 141 (1981).
3. J. E. Dowling and B. Ehinger, *Science* **188**, 270 (1975); ——— and W. L. Hedden, *Invest. Ophthalmol.* **15**, 916 (1976).
4. B. Ehinger and I. Florén, *Cell Tissue Res.* **175**, 37 (1976); *Exp. Eye Res.* **26**, 321 (1978).
5. K. Negishi, *Exp. Eye Res.* **33**, 223 (1981); ———, T. Teranishi, S. Kato, *Acta Histochem. Cytochem.* **14**, 596 (1981).
6. K. Negishi, S. Kato, T. Teranishi, *Neurosci. Lett.* **25**, 1 (1981); K. Negishi *et al.*, *Acta Histochem. Cytochem.* **14**, 449 (1981).
7. K. Negishi, T. Teranishi, S. Kato, *Acta Histochem. Cytochem.* **14**, 654 (1981).
8. We thank N. M. van Gelder for his critical reading of the manuscript and T. Urano for her secretarial and laboratory assistance. Supported in part by a fund from the Johnan Hospital, Takaoka, Japan.

3 November 1981; revised 1 March 1982

Identification of the Constant Chromosome Regions Involved in Human Hematologic Malignant Disease

Abstract. *Specific consistent chromosome translocations are regularly observed in certain human leukemias and lymphomas. For the myeloid leukemias, the constant recombinants are: the long arm of 9 to chromosome 22 in chronic myeloid leukemia, the long arm of 21 to chromosome 8 in acute myeloblastic leukemia, and the long arm of 17 to chromosome 15 in acute promyelocytic leukemia. Three related translocations are seen in Burkitt lymphoma and B cell acute lymphocytic leukemia; in each one, chromosome 8 is involved with chromosome 2, 14, or 22. Analysis of a complex translocation affecting chromosomes 8 and 14 indicates that the translocation of chromosome 8 to chromosome 14 is the critical constant rearrangement. The analysis of the DNA at the translocation sites of these chromosomes, rather than the reciprocal of each translocation, appears to be the most productive focus for initial study. The various immunoglobulin loci are located on chromosomes 2, 14, and 22, the chromosomes regularly involved in translocations in Burkitt lymphoma and B cell acute lymphocytic leukemia.*

Several consistent translocations that are relatively specifically associated with particular types of human leukemia and lymphoma have been identified during the past 8 years (*1*). These include the translocations between chromosomes 9 and 22 in chronic myeloid leukemia (CML) (*2*), between chromosomes 8 and 21 in acute myeloblastic leukemia (AML-M2) (*3*), and between chromosomes 15 and 17 in acute promyelocytic leukemia (APL-M3) (*4*). Three variant translocations, each involving chromosome 8, have been observed in Burkitt lymphoma and acute lymphocytic leukemia (ALL) of B cell origin, which may be two clinical manifestations of the same malignant disease. The three translocations include the one originally identified by Zech *et al.* (*5*) involving chromosomes 8 and 14 (*5*, *6*) as well as two recently described variants, one between 8 and 2 (*7*) and the other between 8 and 22 (*8*). The break point in No. 8 appears to be in the same band in the long arm (8q24) (Fig. 1) in all three translocations. These various translocations appear to be reciprocal; DNA measurements show that there is no gross loss of chromosomal DNA in the 9;22 translocation in CML (*9*).

Interest in defining the DNA sequences at the sites of these translocations has been further stimulated by the recent finding that the three immunoglobulin (Ig) loci, for the heavy chains, the kappa light chain, and the lambda light chain, are each located on one of the three chromosomes involved with No. 8 in these translocations. Thus, the locus for heavy chains is on No. 14 (*10*), that for kappa is on No. 2 (*11*), and that for lambda is on No. 22 (*12*) (Fig. 1). Moreover, with the use of chromosome hybridization in situ, Malcolm *et al.* (*11*) mapped the kappa light chain genes to the short arm of No. 2 (band 2p12–13), the band that is involved in one of the translocations. Finally, Lenoir *et al.* (*13*) reported on the complete concordance of karyotype with the Ig secreted by cells with variant translocations; they have shown that all three tumors with a 2;8 translocation secrete kappa light chains and all seven tumors with an 8;22 translocation secrete lambda light chains.

Recently, the 9;22 translocation has been analyzed with the use of somatic cell hybridization (*14*) and with cloned probes from DNA of sorted human chromosome 22 (*15*). In the interest of increasing the efficiency of the latter experimental approach, it would be useful to distinguish which of the two rearranged chromosomes that result from a reciprocal translocation merits initial detailed analysis. In the myeloid leukemias, the two translocation chromosomes are each involved only with the other in most instances, and there appears to be no reason a priori to choose one recombinant chromosome rather than the other. Fortunately, each of the three common translocations, 9;22 (*1*), 8;21 (*16*), and 15;17 (*17*), also occurs in a variant form in a limited number of patients, and these can be used to determine whether one recombinant chromosome is constant in the variant forms (Fig. 2). For the translocations in AML and APL, one recombinant chromosome is constant and one is variable (the constant one is enclosed in a box in Fig. 2). For CML, the situation is more complex; this may merely reflect the fact that we have data on more than 1100 CML patients whose cells were studied with banding, compared to only about 100 AML patients with 8;21 translocations and 50 to 60 APL patients with a 15;17 translocation. The standard 9;22 translocation occurs in about 92 percent of

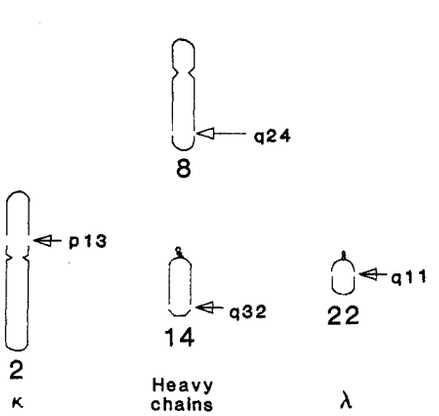

Fig. 1. Diagrammatic representation of the break points (arrows) in the translocations in Burkitt lymphoma and B cell ALL. The short arm of a chromosome is identified by *p* and the long arm by *q*. The kappa light chain (κ) is located on No. 2, the Ig heavy chains on No. 14, and the lambda light chain (λ) on No. 22.

0036-8075/82/0514-0749$01.00/0